Size effects on a two-dimensional hexagonal lattice with application to lithium iodate

P. Tchofo Dinda, E. Coquet, M. Peyrard, and J. M. Crettez
Laboratoire Ondes et Structures Cohérentes, Faculté des Sciences, 6 Boulevard Gabriel, 21000 Dijon, France
(Received 17 July 1991; revised manuscript received 22 October 1991)

We consider a two-dimensional hexagonal nonlinear lattice with two sites per unit cell and an on-site double quadratic potential, which can describe some phase transitions in lithium iodate. We investigate the *strip* version of this model. The phonon stability and phase diagram of this strip-lattice model are determined and compared to those of the *infinite* model to derive size effects on the static structure of the lattice. Furthermore, our phase diagram provides theoretical support for the hypothesis of the existence of an intermediate modification of $LiIO_3$ during the transition from α-$LiIO_3$ to γ-$LiIO_3$.

I. INTRODUCTION

Spatially modulated systems,[1,3–10] domain walls in ferroelectric and antiferroelectric crystals,[2] or phase transitions in various materials such as $LiIO_3$ (Refs. 4, 7, and 8), $NaNO_2$, or $SC(NH_2)$ (Refs. 11–13) have been intensively investigated with various 1D (one-dimensional) and 2D nonlinear lattice models. All the models assume an *infinite* lattice for the determination of the static structure (atomic positions, phase diagram) of the material. Real physical systems, however, are finite, and their surfaces and boundaries can make appreciable contributions to the physical properties of the material. It is notably the case for lithium iodate, where the α-γ transition or even the existence of the γ phase, described in more detail below, depends strongly on the physical state of the material: monocrystal, powder, or grain size in the powders. Neutron-diffraction experiments,[24] performed on powders of $LiIO_3$ with very small grain sizes (less than 20 μm), show that phase-transition temperatures increase as the grain sizes decrease. Furthermore Dénès,[14] who studied phase transitions in SnF_2, has shown that the transition from α-SnF_2 to γ-SnF_2 is greatly influenced by particle size: The transition temperature increases as the grain sizes decrease. Finite-size effects are also observed in specific-heat experiments on phase transitions in monolayers adsorbed at surfaces (e.g., Ne or O_2 adsorbed on grafoil).[15] On the other hand a large amount of theoretical development on critical phenomena in systems with one or more finite dimensions—performed with Ising lattice models.[16–21]—yield some interesting results: Ferdinand and Fisher,[17] who examined some properties of planar-Ising-lattice models, noted the *rounding* and *shifting* of the specific-heat peaks as the size of the lattice decreases. Similar results were also found by Fisher and Barber[16] for the critical temperature of finite-thickness films under boundary conditions. Binder[20] examined finite-size effects on phase transitions in thin films and showed that both first- and second-order transitions get smeared and shifted owing to the finite size of the sample. Thus, size effects play an important role on the physical properties of various materials.

Neutron-diffraction studies of the domain of stability of γ-$LiIO_3$ (Ref. 22) show that γ-$LiIO_3$ is never observed as a single phase but always coexists with α- or β-$LiIO_3$. It is obvious that one cannot rely solely on *infinite* lattice models to derive a bona fide description of the phase diagram for mixed compounds or powders in which several different phases coexist. Therefore, it is interesting—from a theoretical point of view—to include one or more finite dimensions to the nonlinear lattice models[1–10] mentioned earlier.

The purpose of this paper is to take into account the size effects in the study of a 2D nonlinear lattice model, since apart from Ising models all previous 2D nonlinear models assume an infinite lattice for the determination of the phase diagram. The natural and straightforward approach for studying the size effects would be to obtain the phase diagrams for the infinite lattice and the finite lattice, respectively, and then compare the two phase diagrams. However, before considering a 2D model with finite size in both directions of the lattice, an important question that should be answered is how size effects manifest themselves in a 2D model when the lattice size is finite in only one direction, that is, when a material is sensitive to size effects in only one direction of the lattice. We therefore examine the effects of finite sample size on the phonon stability and phase diagram of an hexagonal lattice, which will be made more precise below, with a finite number of cells in one direction and an infinite number of cells in the other, that is, an infinite *strip* with finite width. This simple approach allows us to proceed quite far in the theoretical analysis and facilitate the ensuing numerical calculations. Our phase diagrams show that, in *strip* structures, physical states containing different phases in different grains of a powder are possible, in contrast to the phase diagram of *infinite* lattice models in which the coexistence of different phases occurs solely on the phase-transition lines. The *strip*-lattice model therefore becomes interesting for describing the phase transitions in some powders where phase coexistence is observed experimentally. Such an analysis is also especially interesting for giving an account of some phase transitions, which give rise to a considerable fractioning of the crystals and the occurrence of an amorphous or a very divided phase as an intermediate step in the transition.[14] Such divided phases, made of very small

crystallites, are generally difficult to observe directly *experimentally*. However, their existence has been suggested in some materials such as $LiIO_3$ (Ref. 24) or SnF_2 (Ref. 14). The increase in the phase transition temperatures at smaller grain sizes observed in $LiIO_3$ could be attributed to the smaller probability of nucleation in a small crystallite, but for some materials, such as $BaTiO_3$,[32] the size effects on the phase-transition temperatures are different so that in such cases the sole nucleation process is not sufficient to explain the observed behavior. Therefore a theoretical treatment for *strip*-lattice models can be useful for such cases.

Our theoretical treatment for *strip* structures is relevant, in general, to hexagonal lattices in which two order parameters in each basic cell can occupy two stable equilibrium configurations. In order to illustrate this point we consider as a test case lithium iodate, in which the Li sublattice in the α phase forms an hexagonal lattice and the rotational position of the IO_3^- ions can occupy two stable equilibrium configurations in the enantiomorphic forms of α-$LiIO_3$. Lithium iodate has been intensively investigated in the last few years from an experimental point of view, owing to its piezoelectricity, pyroelectricity, and nonlinear optical physical properties.[23–30] Several distinct crystalline modifications of $LiIO_3$ are known. Two of them, known as α and β phases, are stable at room temperature. Upon heating α-$LiIO_3$ transforms reversibly into γ-$LiIO_3$ (at about 500 K with a large hysteresis), then γ-$LiIO_3$ transforms irreversibly into β-$LiIO_3$ (at 540 K), which is stable up the melting point (768 K). These phases of $LiIO_3$ are discussed in detail in Refs. 23–27. A 2D hexagonal lattice model was developed previously by Coquet, Peyrard, and Büttner[8] to study the phase transitions of $LiIO_3$. In this model the change of the Li sublattice is ignored and attention is focused on the rotation of the IO_3^- ions around the c axis of the crystal, in an a-b plane orthogonal to the c axis. Besides its fundamental interests, this model provides a fairly complete description of the different enantiomorphic forms of α-$LiIO_3$ and gives an account of the α-γ transition of $LiIO_3$.[8] The model describes satisfactorily the phase transitions of $LiIO_3$, which are mainly characterized by the rotation of some IO_3^- ions around the c axis and which do not involve a significant distortion of the Li sublattice, as does the α-γ transition. Coquet, Peyrard, and Büttner[8] have analyzed the phonon stability and examined some quasi-1D phases of the model, and recently a more complete phase diagram[4] including the *true* 2D phases (that is, phases whose periodicity is greater than *one* in the two directions of the lattice) were obtained. In the present paper only such phase transitions are considered. Phase transitions that involve rotations around an axis lying in the a-b plane cannot be described within the present model.

We examine in this paper the static structure of the *strip* version of the 2D hexagonal lattice model. Our calculations for the *strip* model show some typical size effects on this phase diagram.[4] We observe a modification of the phonon stability region, which generates a change in the parameter regions of *high-temperature* phases (that is, the phases that appear near the phonon stability curves). We note that some phases appearing in the *infinite*-lattice phase diagram are no longer the ground states in the *strip* lattices, whereas some other phases become the ground states only in *strip* lattices with small sizes. Furthermore, the phase diagrams that we obtain in this work reveal an intermediate 2D phase whose 3D version has not yet been observed experimentally, which we call ϕ^*, which appears only on the transition line α^*-γ^* for the *infinite* model, and whose domain of existence increases in *strip* lattices. By α^* and γ^* we denote the 2D *version* of α- and γ-$LiIO_3$, respectively, obtained by performing the projection of the structure α and γ onto the a-b plane. The 3D version of ϕ^* is therefore suggested by our treatment of *strip* structures as an intermediate modification of $LiIO_3$ during the transition α-γ. This hypothesis has been already suggested by Crettez *et al.*,[24] who performed neutron-powder-diffraction patterns of $(\alpha+\gamma)$- and β-phase lithium iodate. Their results suggest that the transition from α to γ proceeds through an intermediate phase, which may well be amorphous or at least a very divided phase.

The paper is organized as follows: In the following section we present the calculational procedure for obtaining the commensurate static solutions for the atomic positions in the strip lattices. In Sec. III we perform the phonon stability and the phase-diagram analysis for the *strip* structures, and we derive size effects on the static structure of the lattice. In the last section we summarize all results of the paper. Our investigation consists of analytic as well as numerical calculations. These calculations treat intrinsically the discreteness of the lattice.

II. GENERAL STATIC SOLUTIONS

The model is schematically shown in Fig. 1. Two sites $i=1,2$ lie at positions $(\frac{2}{3},\frac{1}{3})$, $(\frac{1}{3},\frac{2}{3})$ in each cell. The cells are labeled by indices n,m and the sites by n,m,i. The lattice is infinite in the m direction and consists of N sites in the n direction, ranging from 0 to $N-1$. Each site is characterized by an order parameter $q_{n,m,i}$, which represents the rotational position of an iodate ion of $LiIO_3$. To take into account the two possible positions of the IO_3^- ion observed in the enantiomorphic forms of

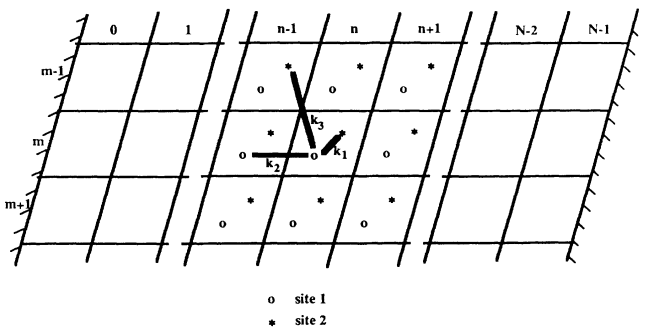

FIG. 1. The *strip* version of the 2D hexagonal lattice model under consideration.

the α phase, an on-site potential with a double quadratic form is assumed:

$$V_p=\tfrac{1}{2}\mu^2(q_{n,m,i}-\varepsilon\sigma_{n,m,i})^2$$

(for a site n,m,i), where $\sigma_{n,m,i}=\mathrm{sgn}(q_{n,m,i})$, μ^2 measures the potential barrier, and $\pm\varepsilon$ locates the two minima of the potential. A site n,m,i situated in the bulk of the system ($1\le n\le N-2$) is connected to neighboring sites by harmonic interactions of constant k_1 for the three nearest neighbors of the second type, k_2 with the six nearest neighbors of the same type i, and k_3 with the three second neighbors of the opposite type so that the energy per site for two sites in the cell n,m situated in the bulk of the system is

$$\begin{aligned}
f_{n,m,1}=&\tfrac{1}{2}\mu^2(q_{n,m,1}-\varepsilon\sigma_{n,m,1})^2\\
&+\tfrac{1}{4}k_1[(q_{n,m,1}-q_{n,m,2})^2+(q_{n,m,1}-q_{n,m-1,2})^2+(q_{n,m,1}-q_{n+1,m,2})^2]\\
&+\tfrac{1}{4}k_2[(q_{n,m,1}-q_{n-1,m,1})^2+(q_{n,m,1}-q_{n-1,m-1,1})^2+(q_{n,m,1}-q_{n,m-1,1})^2\\
&+(q_{n,m,1}-q_{n+1,m,1})^2+(q_{n,m,1}-q_{n+1,m+1,1})^2+(q_{n,m,1}-q_{n,m+1,1})^2]\\
&+\tfrac{1}{4}k_3[(q_{n,m,1}-q_{n-1,m-1,2})^2+(q_{n,m,1}-q_{n+1,m-1,2})^2+(q_{n,m,1}+q_{n+1,m+1,2})^2]\ ,\\
f_{n,m,2}=&\tfrac{1}{2}\mu^2(q_{n,m,2}-\varepsilon\sigma_{n,m,2})^2\\
&+\tfrac{1}{4}k_1[(q_{n,m,2}-q_{n,m,1})^2+(q_{n,m,2}-q_{n,m+1,1})^2+(q_{n,m,2}-q_{n-1,m,1})^2]\\
&+\tfrac{1}{4}k_2[(q_{n,m,2}-q_{n-1,m,2})^2+(q_{n,m,2}-q_{n-1,m-1,2})^2+(q_{n,m,2}-q_{n,m-1,2})^2\\
&+(q_{n,m,2}-q_{n+1,m,2})^2+(q_{n,m,2}-q_{n+1,m+1,2})^2+(q_{n,m,2}-q_{n,m+1,2})^2]\\
&+\tfrac{1}{4}k_3[(q_{n,m,2}-q_{n-1,m+1,1})^2+(q_{n,m,2}-q_{n-1,m-1,2})^2+(q_{n,m,2}-q_{n+1,m+1,1})^2]\ .
\end{aligned}$$

We have used here a symmetrized form of the energy per site in which half the coupling energy of a site with its neighbors is introduced—hence the factor $\frac{1}{4}$. The energy per cell n,m in the bulk of the structure is then

$$f_{n,m}=f_{n,m,1}+f_{n,m,2}\ . \tag{2.1}$$

These expressions are formally equivalent to those of the infinite lattice; however, they must be modified in order to correctly describe the system behavior at the free edges of the lattice. Thus,

$$f_{0,m}=f_{0,m,1}+f_{0,m,2}\ , \tag{2.2}$$

where $f_{0,m,1}$ and $f_{0,m,2}$ are obtained from the general expressions by removing the interactions with the $n-1,m$ sites (and replacing n by 0). In a similar manner on the other side of the lattice

$$f_{N-1,m}=f_{N-1,m,1}+f_{N-1,m,2} \tag{2.3}$$

is obtained by eliminating the interactions involving the $n+1,m$ sites. The total energy of the system is then

$$F=\sum_m\sum_{n=0}^{n=N-1}f_{n,m}\ . \tag{2.4}$$

The static structure of the system is obtained by energy minimization, which gives the following equilibrium equations for each site.

For $n=1,2,\ldots,N-2$:

$$\begin{aligned}
&[\mu^2+3(k_1+k_3)+6k_2]q_{n,m,1}-k_1(q_{n,m,2}+q_{n,m-1,2}+q_{n+1,m,2})\\
&\qquad-k_2(q_{n-1,m,1}+q_{n-1,m-1,1}+q_{n,m-1,1}+q_{n+1,m,1}+q_{n+1,m+1,1}+q_{n,m+1,1})\\
&\qquad-k_3(q_{n-1,m-1,2}+q_{n+1,m-1,2}+q_{n+1,m+1,2})=\varepsilon\mu^2\sigma_{n,m,1}\ ,
\end{aligned} \tag{2.5a}$$

$$\begin{aligned}
&[\mu^2+3(k_1+k_3)+6k_2]q_{n,m,2}-k_1(q_{n,m,1}+q_{n,m+1,1}+q_{n-1,m,1})\\
&\qquad-k_2(q_{n-1,m,2}+q_{n-1,m-1,2}+q_{n,m-1,2}+q_{n+1,m,2}+q_{n+1,m+1,2}+q_{n,m+1,2})\\
&\qquad-k_3(q_{n-1,m-1,1}+q_{n+1,m+1,1}+q_{n-1,m+1,1})=\varepsilon\mu^2\sigma_{n,m,2}\ .
\end{aligned} \tag{2.5b}$$

For $n=0$

$$\begin{aligned}
&(\mu^2+3k_1+4k_2+2k_3)q_{0,m,1}-k_1(q_{0,m,2}+q_{0,m-1,2}+q_{1,m,2})-k_3(q_{1,m-1,2}+q_{1,m+1,2})\\
&\qquad-k_2(q_{0,m-1,1}+q_{1,m,1}+q_{1,m+1,1}+q_{0,m+1,1})=\varepsilon\mu^2\sigma_{0,m,1}\ ,
\end{aligned} \tag{2.6a}$$

$$(\mu^2+2k_1+4k_2+k_3)q_{0,m,2}-k_1(q_{0,m,1}+q_{0,m+1,1})-k_3q_{1,m+1,1}$$
$$-k_2(q_{0,m-1,2}+q_{1,m,2}+q_{1,m+1,2}+q_{0,m+1,2})=\varepsilon\mu^2\sigma_{0,m,2}\ . \quad (2.6b)$$

For $n=N-1$

$$(\mu^2+2k_1+4k_2+k_3)q_{N-1,m,1}-k_1(q_{N-1,m,2}+q_{N-1,m-1,2})-k_3q_{N-2,m-1,2}$$
$$-k_2(q_{N-2,m,1}+q_{N-2,m-1,1}+q_{N-1,m-1,1}+q_{N-1,m+1,1})=\varepsilon\mu^2\sigma_{N-1,m,1}\ , \quad (2.7a)$$

$$(\mu^2+3k_1+4k_2+2k_3)q_{N-1,m,2}-k_1(q_{N-1,m,1}+q_{N-1,m+1,1}+q_{N-2,m,1})$$
$$-k_2(q_{N-2,m,2}+q_{N-2,m-1,2}+q_{N-1,m-1,2}+q_{N-1,m+1,2})-k_3(q_{N-2,m-1,1}+q_{N-2,m+1,1})=\varepsilon\mu^2\sigma_{N-1,m,2}\ . \quad (2.7b)$$

It is important to notice that in the *infinite* lattice each phase is characterized by its periodicity in the two infinite directions of the lattice, whereas in the *strip* lattice the periodicity cannot be defined in the finite direction n. Thus, the essential parameters to consider in calculating the static solutions of a *strip* lattice are N and P_m. For a given phase with periodicity P_m in m and configuration σ, embedded in a *strip* lattice with size N in n, we rewrite the equilibrium equations (2.5), (2.6), and (2.7) with the periodicity condition

$$q_{n,m,i}=q_{n,m+P_m,i}\ , \quad (2.8)$$

which gives us systems of equations that we rewrite in the following matrix form:

$$B^{(0)}_{P_m}U_{0,P_m}+A^T_{P_m}U_{1,P_m}=D_{0,P_m}\ ; \quad (2.9)$$

$$A_{P_m}U_{n-1,P_m}+B_{P_m}U_{n,P_m}+A^T_{P_m}U_{n+1,P_m}=D_{n,P_m},\ \text{for } n=1,2,\ldots,N-2\ ; \quad (2.10)$$

$$A_{P_m}U_{N-2,P_m}+B^{(1)}_{P_m}U_{N-1,P_m}=D_{N-1,P_m}\ ; \quad (2.11)$$

where U_{n,P_m} and D_{n,P_m} are the following $2P_m\times 1$ (column) matrices, respectively, for the atomic positions and the configuration σ:

$$U_{n,P_m}=\begin{bmatrix} q_{n,0,1}\\ q_{n,0,2}\\ q_{n,1,1}\\ q_{n,1,2}\\ \vdots\\ q_{n,P_m-1,1}\\ q_{n,P_m-1,2}\end{bmatrix},\quad D_{n,P_m}=\varepsilon\mu^2\begin{bmatrix} \sigma_{n,0,1}\\ \sigma_{n,0,2}\\ \sigma_{n,1,1}\\ \sigma_{n,1,2}\\ \vdots\\ \sigma_{n,P_m-1,1}\\ \sigma_{n,P_m-1,2}\end{bmatrix}. \quad (2.12)$$

The superscript T denotes the transposed matrix; $B^{(0)}_{P_m}$, A_{P_m}, B_{P_m}, and $B^{(1)}_{P_m}$ are $2P_m\times 2P_m$ matrices (an $n\times m$ matrix is taken to mean a matrix with n rows and m columns), defined as follows:

$$B^{(0)}_1=\begin{bmatrix}\mu^2+2(k_1+k_2)+k_3 & -2k_1\\ -2k_1 & \mu^2+3k_1+2(k_2+k_3)\end{bmatrix}, \quad (2.13a)$$

$$A_1=\begin{bmatrix}-2k_2 & -(k_1+2k_3)\\ -k_3 & -2k_2\end{bmatrix},$$

$$B_1=\begin{bmatrix}\mu^2+3(k_1+k_3)+4k_2 & -2k_1\\ -2k_1 & \mu^3+3(k_1+k_3)+4k_2\end{bmatrix}, \quad (2.13b)$$

$$B^{(1)}_1=\begin{bmatrix}\mu^2+3k_1+2(k_2+k_3) & -2k_1\\ -2k_1 & \mu^2+2(k_1+k_2)+k_3\end{bmatrix}, \quad (2.13c)$$

$$B^{(0)}_2=\begin{bmatrix}\delta_0 & -k_1 & -2k_2 & -k_1\\ -k_1 & \rho_0 & -k_1 & -2k_2\\ -2k_2 & -k_1 & \delta_0 & -k_1\\ -k_1 & -2k_2 & -k_1 & \rho_0\end{bmatrix}. \quad (2.14a)$$

$B^{(1)}_2$ has the same form as $B^{(0)}_2$, but with δ_0 and ρ_0 interchanged:

$$A_2=\begin{bmatrix}-k_2 & 0 & -k_2 & -k_3\\ -k_1 & -k_2 & -2k_3 & -k_2\\ -k_2 & -k_3 & -k_2 & 0\\ -2k_3 & -k_2 & -k_1 & -k_2\end{bmatrix},$$

$$B_2=\begin{bmatrix}\delta & -k_1 & -2k_2 & -k_1\\ -k_1 & \delta & -k_1 & -2k_2\\ -2k_2 & -k_1 & \delta & -k_1\\ -k_1 & -2k_2 & -k_1 & \delta\end{bmatrix}, \quad (2.14b)$$

with

$$\delta_0=\mu^2+3k_1+4k_2+2k_3\ ,$$
$$\rho_0=\mu^2+2k_1+4k_2+k_3\ , \quad (2.15)$$
$$\delta=\mu^2+3(k_1+k_3)+6k_2\ .$$

From $P_m=3$ upwards, the order of $B^{(0)}_{P_m}$, A_{P_m}, B_{P_m},

and $B_{P_m}^{(1)}$ becomes increasingly large so that it becomes more convenient to express these matrices in block form. Indeed, expressing the matrices $B_{P_m}^{(0)}$, A_{P_m}, B_{P_m}, and $B_{P_m}^{(1)}$, for $P_m \geq 3$, as $P_m \times P_m$ matrices whose elements are 2×2 submatrices, we find that they have the same general expression as the matrix $\psi_j(x_1,x_2,x_3)$ given in Table I, where by x_1,x_2,x_3 we denote *nonzero* 2×2 submatrices and the subscript j indicates the order of ψ_j (ψ_j is a $j\times j$ matrix). Thus, each of the matrices $B_{P_m}^{(0)}$, A_{P_m}, B_{P_m}, and $B_{P_m}^{(1)}$ is now determined by a unique set of three 2×2 submatrices x_1,x_2,x_3 for all $P_m \geq 3$. In this notation these matrices have a simple form:

$$B_{P_m}^{(0)}=\psi_{P_m}(b_1,b_0,b_1^T), \quad B_{P_m}^{(1)}=\psi_{P_m}(b_1,\bar{b}_0,b_1^T) , \tag{2.16a}$$

$$A_{P_m}=\psi_{P_m}(a_1,a_2,a_3), \quad B_{P_m}=\psi_{P_m}(b_1,b,b_1^T) , \tag{2.16b}$$

where

$$b_1=\begin{bmatrix} -k_2 & -k_1 \\ 0 & -k_2 \end{bmatrix},$$

$$b_0=\begin{bmatrix} \delta_0 & -k_1 \\ -k_1 & \rho_0 \end{bmatrix}, \tag{2.17a}$$

$$b=\begin{bmatrix} \delta & -k_1 \\ -k_1 & \delta \end{bmatrix},$$

$$a_1=\begin{bmatrix} -k_2 & -k_3 \\ -k_3 & -k_2 \end{bmatrix},$$

$$a_2=\begin{bmatrix} -k_2 & 0 \\ -k_1 & -k_2 \end{bmatrix}, \tag{2.17b}$$

$$a_3=\begin{bmatrix} 0 & 0 \\ -k_3 & 0 \end{bmatrix}.$$

$\bar{b}_0$ has the same form as b_0, but with δ_0 and ρ_0 interchanged.

Equations (2.9), (2.10), and (2.11) form a tridiagonal system for matrices. We then solve these equations using the well-known recursive Choleski method,[31] which we have extended to work with matrices instead of numbers. Thus, we introduce the recursion solution—at order n—of the form:

$$U_{n,P_m}=S_{n,P_m}+T_{n,P_m}U_{n+1,P_m} , \tag{2.18}$$

TABLE I. General expression of matrix $\psi_j(x_1,x_2,x_3)$, of order j. Each element of $\psi_j(x_1,x_2,x_3)$ is a 2×2 submatrix, and x_1, x_2, and x_3 denote *nonzero* submatrices.

$$\psi_j(x_1,x_2,x_3)=\begin{bmatrix} x_2 & x_3 & 0 & \cdots & 0 & 0 & x_1 \\ x_1 & x_2 & x_3 & 0 & \cdots & 0 & 0 \\ 0 & x_1 & x_2 & x_3 & 0 & \cdots & 0 \\ \vdots & \ddots & \ddots & \ddots & \ddots & \ddots & \vdots \\ 0 & \cdots & 0 & x_1 & x_2 & x_3 & 0 \\ 0 & 0 & \cdots & 0 & x_1 & x_2 & x_3 \\ x_3 & 0 & 0 & \cdots & 0 & x_1 & x_2 \end{bmatrix}$$

in which the matrices S_{n,P_m} and T_{n,P_m} are to be determined. Substitution of Eq. (2.18)—at order $n-1$—into the nth equation (2.10) yields the relationship between U_{n,P_m} and U_{n+1,P_m} in (2.18), subjected to the following recursion relations:

$$S_{n,P_m}=(A_{P_m}T_{n-1,P_m}+B_{P_m})^{-1}(D_{n,P_m}-A_{P_m}S_{n-1,P_m}) \tag{2.19a}$$

$$T_{n,P_m}=-(A_{P_m}T_{n-1,P_m}+B_{P_m})^{-1}A_{P_m}^T \quad (n=1,2,\ldots,N-2) . \tag{2.19b}$$

Also, from Eq. (2.9), one straightforwardly obtains

$$S_{0,P_m}=(B_{P_m}^{(0)})^{-1}D_{0,P_m}, \quad T_{0,P_m}=-(B_{P_m}^{(0)})^{-1}A_{P_m}^T . \tag{2.20}$$

Finally, substitution of the solution (2.18)—at order $N-2$—into Eq. (2.11) yields

$$U_{N-1,P_m}=(A_{P_m}T_{n-2,P_m}+B_{P_m}^1)^{-1} \times(D_{n-1,P_m}-A_{P_m}S_{N-2,P_m})=S_{N-1,P_m} . \tag{2.21}$$

We stress that this calculational procedure—using the following two-step process—enables us to obtain all the commensurate static solutions for an *N-strip* lattice (i.e., with size N in n).

(i) We first calculate all the S_{n,P_m}'s and T_{n,P_m}'s using, successively, the recursion formulas (2.20), (2.19a), (2.19b), and (2.21) (in this order). Note that Eq. (2.21) also gives us, straightforwardly, U_{N-1,P_m}.

(ii) Next, we make use of Eq. (2.18), with n ranging from $N-2$ to 0, to obtain the others U_{n,P_m}'s. The static solutions $q_{n,m,i}$ must, of course, be checked for self-consistency at each site. The self-consistency conditions are written as

$$\sigma_{n,m,i}=\mathrm{sgn}(q_{n,m,i}) , \tag{2.22}$$

so that if Eq. (2.22) is not fulfilled, the corresponding solution is not valid. We now consider the phase diagram for the *strip* lattice.

III. PHASE DIAGRAMS

A. Phonon stability analysis

For a nonlinear lattice the phonon stability generally depends upon the particular phase that is considered. This is not the case for our model, owing to the piecewise harmonic double-well potential. Thus, a general investigation of phonon stability analysis for our system can now be performed. Furthermore, we recall that the *infinite* lattice is a system with two degrees of freedom in a cell n,m, so that the eigenfrequencies for the small amplitude displacements of the form

$$y_{n,m,i}=Y_i\exp(j\omega t)\exp[-j(nQ_1+mQ_2)] , \tag{3.1}$$

near the equilibrium configuration ($q_{n,m,1}=q^0_{n,m,1}$) in a given phase, ω_1^2 and ω_2^2, depend upon the model parameters and the components Q_1 and Q_2 of a wave vector $\mathbf{Q}=Q_1\mathbf{a}+Q_2\mathbf{b}$ in the first Brillouin zone. The squares of the frequencies, ω_1^2 and ω_2^2, have been previously obtained by Coquet, Peyrard, and Büttner.[8] Thus, for a given parameter set k_1,k_2,k_3,μ^2, the *infinite* lattice is linearly stable if the two eigenfrequencies ω_1^2 and ω_2^2 are positive for all $\mathbf{Q}$ in the first Brillouin zone. Owing to the finite size in the n direction, the basic cell of an *N-strip* lattice is, in fact, a row of N cells n,m in the n direction. This *strip* lattice gives, therefore, a system with $2N$ degrees of freedom per basic cell. We then look for solutions of the form of small amplitude displacements near the equilibrium configuration

$$q_{n,m,1}=q^0_{n,m,1}+x_{n,1}\exp(j\omega t)\exp(-jmQ)\ , \tag{3.2a}$$

$$q_{n,m,2}=q^0_{n,m,2}+x_{n,2}\exp(j\omega t)\exp(-jmQ)\ , \tag{3.2b}$$

in which Q is the component of a wave vector $\mathbf{Q}=Q\mathbf{a}$ in the first Brillouin zone. The squares of the frequencies ω_i^2 ($i=1,2,\ldots,2N$) are given by the eigenvalues of the following $2N\times 2N$ matrix P:

$$P=\begin{pmatrix} P_{1,1} & P_{1,2} \\ (P^T_{1,2})^* & P_{2,2} \end{pmatrix} \tag{3.3}$$

with

$$P_{1,1}=\begin{pmatrix} \vartheta_0 & \chi^* & 0 & \cdots & 0 & 0 & 0 \\ \chi & \vartheta & \chi^* & 0 & \cdots & 0 & 0 \\ 0 & \chi & \vartheta & \chi^* & 0 & \cdots & 0 \\ \vdots & \ddots & \ddots & \ddots & \ddots & \ddots & \cdots \\ 0 & \cdots & 0 & \chi & \vartheta & \chi^* & 0 \\ 0 & 0 & \cdots & 0 & \chi & \vartheta & \chi^* \\ 0 & 0 & 0 & \cdots & 0 & \chi & \vartheta_1 \end{pmatrix}, \tag{3.4}$$

$$P_{1,2}=\begin{pmatrix} \xi & \lambda & 0 & \cdots & 0 & 0 & 0 \\ \eta & \xi & \lambda & 0 & \cdots & 0 & 0 \\ 0 & \eta & \xi & \lambda & 0 & \cdots & 0 \\ \vdots & \ddots & \ddots & \ddots & \ddots & \ddots & \vdots \\ 0 & \cdots & 0 & \eta & \xi & \lambda & 0 \\ 0 & 0 & \cdots & 0 & \eta & \xi & \lambda \\ 0 & 0 & 0 & \cdots & 0 & \eta & \xi \end{pmatrix}.$$

In these expressions the superscript "*" designates the complex conjugate,

$$\vartheta_0=\mu^2+3k_1+2k_3+2k_2(2-\cos Q)\ ,$$

$$\vartheta_1=\mu^2+2k_1+k_3+2k_2(2-\cos Q)\ ,$$

$$\vartheta=\mu^2+3k_1+3k_3+2k_2(3-\cos Q)\ ,$$

$$\chi=-k_2[1+\exp(jQ)],\quad \eta=-k_3\exp(jQ)\ ,$$

$$\xi=-k_1[1+\exp(jQ)],\quad \lambda=-(k_1+2k_3\cos Q)\ .$$

$P_{2,2}$ has the same form as $P_{1,1}$, but with ϑ_0 and ϑ_1 interchanged.

Thus, for a given parameter set, the stability condition for an *N-strip* lattice is written as

$$\omega_i^2>0,\quad \text{for } i=1,2,\ldots,2N,\quad \text{and for all } \mathbf{Q}\ . \tag{3.5}$$

Note that the condition (3.5) depends not only on the model parameters, but also on the size of the lattice in the

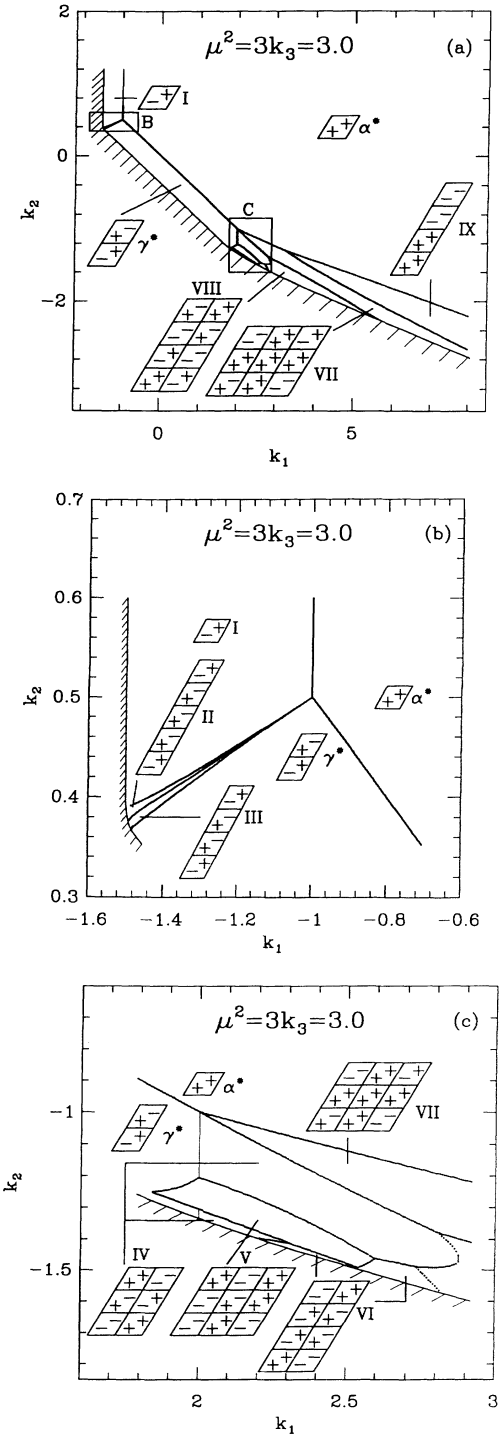

FIG. 2. Plot of the phase diagram of the *infinite* lattice obtained by Tchofo Dinda and Coquet (Ref. 4). (b) and (c) are enlargements of the small boxes *B* and *C*, respectively, shown in (a).

finite direction of the lattice. In Fig. 2(a) the shaded border indicates the stability curve for the *infinite* lattice, obtained by Coquet, Peyrard, and Büttner.[8] This curve consists entirely of straight lines with sharp intersections. It has been shown in Ref. 8 that in the domain of the parameter space that appears in Fig. 2(a) the model provides the best qualitative description of the α-γ transition of $LiIO_3$. The same domain of the parameter space was subsequently used[4] for performing a more complete analysis of the phase diagram from a theoretical point of view. We consider in the present paper the same domain in the parameter space in order to make the connection with previous work[4,8] and, hence, facilitate the comparison with the findings of previous work[4,8] and our *strip calculation* of phases. We determine the stability curves for the *N-strip* lattices, from $N=10$ upwards. Figures 3, 4, and 5 show the stability curves for $N=10$, 11, 40, 41, 80, and 81, indicated by the shaded borders in the figures. The reasons for choosing those values of N are given in the following section. Size effects on the phonon stability become evident when these stability curves are compared with that of the *infinite* lattice in Fig. 2(a). As general result, we observe a *rounding* of the sharp intersections of straight lines (that are present in the stability curve of the *infinite* lattice) as the size N of the lattice decreases. Furthermore, all the stability curves (for the values of N considered) essentially lie entirely in the phonon stability region of the *infinite* lattice. For lower N values, the stability curves have a paraboliclike shape (Fig. 3). As N increases, these curves progressively collapse on the stability curve of the *infinite* lattice. These curves, for higher N values, consist of straight lines (very close to those of the *infinite* lattice) connected by smooth intersections. The fact that these intersections are still round for $N=80$ simply implies that for the corresponding parameter regions the value of N chosen is not yet sufficient to induce an *infinitelike* behavior. Furthermore, we stress that the shift in the curves as a function of the size N is very slow so that it is only slightly visible in Figs. 3, 4, and 5, which indicates that these systems are in states that are extremely sensitive to boundary effects, even if the boundaries are at very large distance apart. As a result of the modification of the stability curve in the *strip* lattices, the domain of existence of high-temperature phases (those are phases that appear near the stability curve in the phase diagram) is modified and shifted. We now consider the phase diagrams.

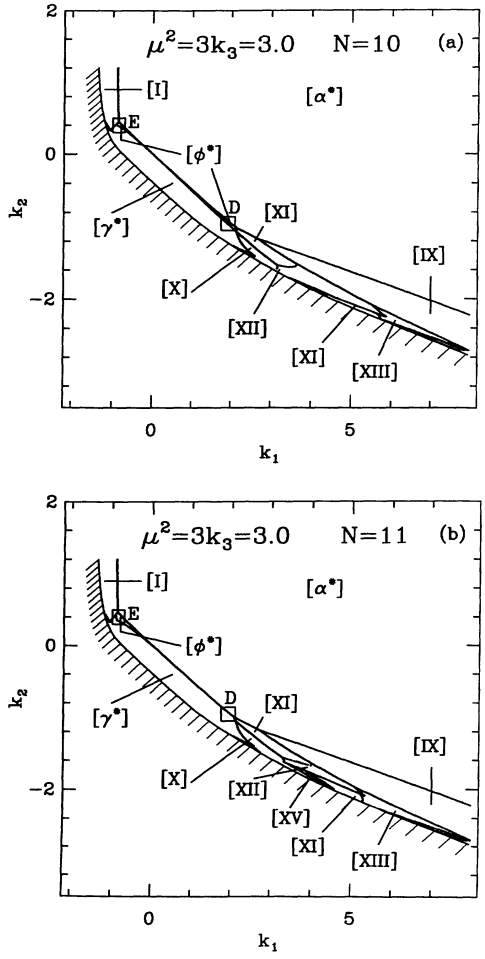

FIG. 3. Plot of the phase diagram of the *strip* lattices for $\mu^2=3k_1=3$, $N=10$ (a) and $N=11$ (b).

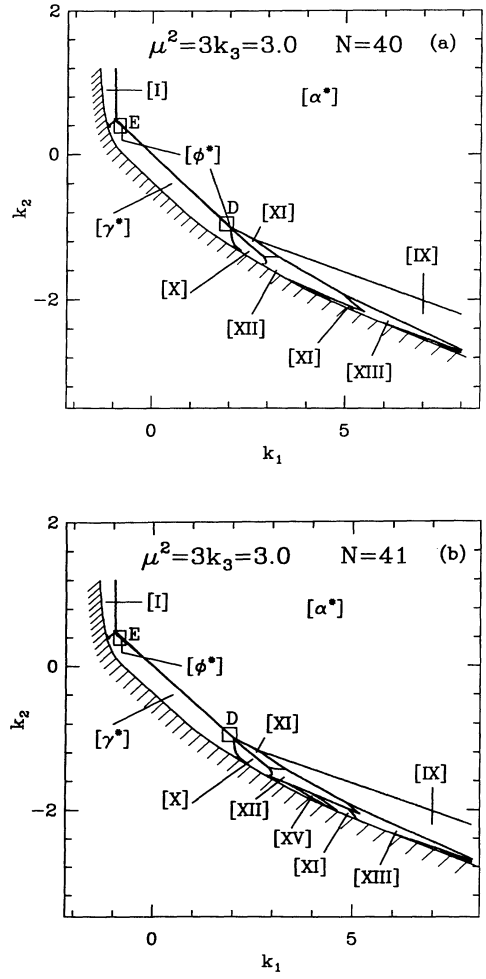

FIG. 4. Plot of the phase diagram of the *strip* lattices for $\mu^2=3k_1=3$, $N=40$, (a) and $N=41$ (b).

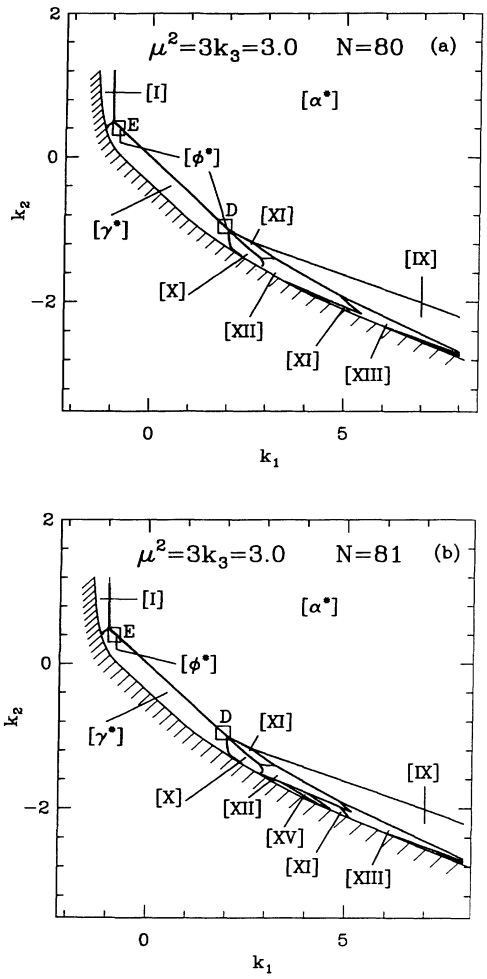

FIG. 5. Plot of the phase diagram of the *strip* lattices for $\mu^2=3k_1=3$, $N=80$ (a) and $N=81$ (b).

B. Ground states

As mentioned earlier, we emphasize that a periodicity can be defined only in the infinite direction m of an *N-strip* lattice, so that the unit cell of a periodic structure with period P_m in an *N-strip* lattice consists of a group of NP_m cells n,m embedded in the *strip*. Since our approach looks for periodic structures, hereafter only the unit cells of commensurate phases will be considered. For each of these unit cells there exists altogether 2^{2NP_m} possible configurations σ, which are candidates for the ground state for a given parameter set. Only some of them correspond to energetically different phases because of symmetry reasons. However, since the possible periods P_m range from unity to infinity (incommensurate phases), there are, in fact, an infinite number of possible configurations, which are candidates for the ground states. Since we are interested in size effects on the phase diagram, we consider in this work the *strip versions* of some commensurate phases that we considered recently for studying the *infinite* lattice. In order to indicate precisely what we mean by the *strip version* of a commensurate phase of the *infinite* lattice, let us introduce some notations that will make the discussions more clear. By "$R*S$ phase" we denote a commensurate phase of the *infinite* lattice with periodicity R in n and S in m. By $[\sigma]_{l_n,l_m}$ we designate the configuration of a group of $l_n l_m$ cells n,m embedded in an *infinite* or *strip* lattice. We build up the configuration of the unit cell of the *strip version* of a commensurate phase $R*S$ by setting a succession of identical building blocks $[\sigma]_{R,S}$ along the n direction, across the *strip* lattice. It is important to note that in the *infinite* lattice the directions n and m are strictly equivalent so that a commensurate phase $[\sigma]_{R,S}$ is the same phase as $[\sigma]_{S,R}$ obtained by simply interchanging the n and m axes. So if $R\neq S$, then two different configurations for the *strip version* of $[\sigma]_{R,S}$ ($\equiv[\sigma]_{S,R}$) can be constructed depending upon the way the building blocks are disposed along n in an *N-strip* lattice. If one disposes the building block $[\sigma]_{R,S}$ along n in a way such that the period of the commensurate *strip version* P_m is equal to R, then the number of identical blocks within the unit cell constructed will be $h_1=\text{int}(N/S)$, where "int(x)" designates the integral part of x. In order to facilitate some forthcoming discussions, we treat S as a *pseudoperiod* in n, denoted P_n^*. On the other hand, if one disposes the building blocks so that $P_m=S$ ($P_n^*=R$), that will yield $h_2=\text{int}(N/R)$ identical blocks within the unit cell of the *strip* lattices then constructed. For performing the phase diagrams we systematically consider that of these two commensurate *strip versions,* which corresponds to the largest number of identical building blocks per unit cell (i.e., the lowest *pseudoperiod* P_n^*). This choice allows us to treat *strip* lattices with relatively lower N values (which is advantageous for numerical computations), and which contain enough identical building blocks to exhibit bona fide size effects. Furthermore, for the forthcoming discussions we denote the commensurate phase of the *infinite* lattice by Roman numerals, and the commensurate *strip version* of a phase J ("J" is a Roman numeral) as $[J]_{N,h}$, where N and h refer, respectively, to the size of the lattice in n and the number of identical building blocks per unit cell. In plotting the phase diagrams we use the notation $[J]$ instead of $[J]_{N,h}$ for simplicity.

In order to facilitate the comparison between the phase diagram of the infinite lattice and that of the strip lattice, we consider the *strip* versions of the 140 phases that we examined recently in performing the phase diagram for the *infinite* lattice.[4] In this reference all the centrosymmetric configurations and those with an inversion center, with the following periodicities are considered: $1*1$, $1*2$, $1*3$, $1*4$, $1*5$, $2*2$, $2*3$, $2*4$, and $3*3$. This is largely sufficient to draw most of the interesting conclusions for $LiIO_3$ for which only phases with low periods are known. However, it should be mentioned that the restriction to those phases does not exclude the possibility of the existence of higher-period phases or even the incommensurate phases. However, such phases generally occupy very small parameter regions when they appear in a phase diagram (compared to the region occupied by lower-period phases) for double-quadratic systems.[1,3,4,5,8] Furthermore, it is obvious that the phase diagrams for

different N values have to be considered to obtain a bona fide description of a powder, where one can find different N values (for the *strip* lattices) even for a given average grain size. Figures 3, 4, and 5, where only phases that occupy the larger regions in the phase diagrams are mentioned, show the results obtained for $N=10$, 11, 40, 41, 80, and 81. As general results we find that the *strip versions* of some phases that are present in the phase diagram of the *infinite* lattice also appear as ground states in the phase diagram for the *strip* lattices. Those are phases α^*, γ^*, ϕ^* (see the discussion below for the reason why ϕ^* is not visible in Fig. 2), I and IX. The configuration of ϕ^* is given in Table II. On the other hand, some quasi-1D and *true* 2D phases, which are not present in the phase diagram of the *infinite* lattice, become the ground states in some parameter regions for the *strip* lattice. Those are phases [X], [XI], [XII], [XIII], and [XV]. The configurations of their corresponding *infinite* versions are given in Table II. Furthermore, we stress that with the exception of phase ϕ^* the *strip* versions of the *true* 2D phases, which are present in the *infinite* lattice do not appear as ground states in the *strip* lattices because of self-consistency reasons. This suggests that the *true* 2D phases are much more sensitive to size effects than the quasi-1D phases.

We now discuss in more detail some interesting results. We first comment on size effects on phases α^*, γ^*, $[\phi^*]$, and the α^*-γ^* transition. We point out that in the phase diagram for the *infinite* lattice (Fig. 2), in fact, in addition to α^* and γ^* another phase also exists along the α^*-γ^* transition line. That is phase ϕ^*. Note that the orthohexagonal unit cell of this phase consists of the juxtaposition of the orthohexagonal unit cells of the its two adjacent phases α^* and γ^*. This intermediate phase has not been revealed in previous work.[4,8] Furthermore, Figs. 6 and 7 giving plots of the energies of phases $[\alpha^*]$, $[\gamma^*]$, and $[\phi]^*$ as a function of N better illustrate size effects on these phases in the transition regions between $[\alpha^*]$ and $[\gamma^*]$. Note that the energy of $[\alpha^*]$, represented by the horizontal straight line in Fig. 7, is always zero owing to the fact that the $[\alpha^*]$ phase lattice is always equivalent—with regard to its static structure (atomic positions)—to a fictitious lattice where the interactions between sites do not exist ($k_1=k_2=k_3=0$). In this fictitious lattice all the *atoms* lie naturally in the same equilibrium position $q_{n,m,i}=\varepsilon$ representing one of the minima of the local potential (which corresponds to a zero total energy). Therefore, size effects—which result in some missing couplings at the free edges of the lattices—do not affect the static structure of this lattice. Furthermore, we also see in Figs. 6 and 7 that the energy curves of $[\phi^*]$ versus N oscillates. We think that this energy oscillates because in $[\phi^*]$ the *pseudoperiod* is $P_n^*=2$ (and $P_m=2$), and therefore two types of *N-strip* lattices $[\phi^*]_{N,h}$ can be constructed depending on whether N is even or odd, corresponding, respectively, to $\mathrm{mod}(N,h)=0$ and $\mathrm{mod}(N,h)=\frac{1}{2}$ [$\mathrm{mod}(N,h)$ designates the remain of the division of N by h]. The two envelope curves of these oscillations correspond precisely to $\mathrm{mod}(N,h)=0$ and $\mathrm{mod}(N,h)=\frac{1}{2}$, respectively. Also note that $P_n^*=1$ in the *strip* structures corresponding to quasi-1D phases of the *infinite* lattice, and consequently only one type of the *N-strip* lattices "$[\mathrm{J}]_{N,h}$" corresponding to $\mathrm{mod}(N,h)=\mathrm{mod}(N,N)=0$ can be constructed, for all N. That is the reason for which the energy of $[\gamma]^*$ versus N

TABLE II. Configuration of phase ϕ^* and the commensurate phases which are not present in the phase diagram of the *infinite* lattice, whose *strip* versions are the ground states in some parameter regions in the phase diagrams for *strip* lattices in Figs. 3, 4, and 5.

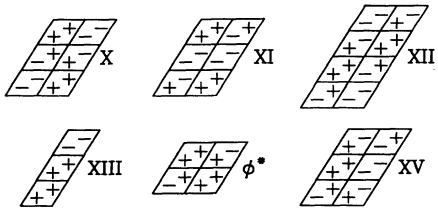

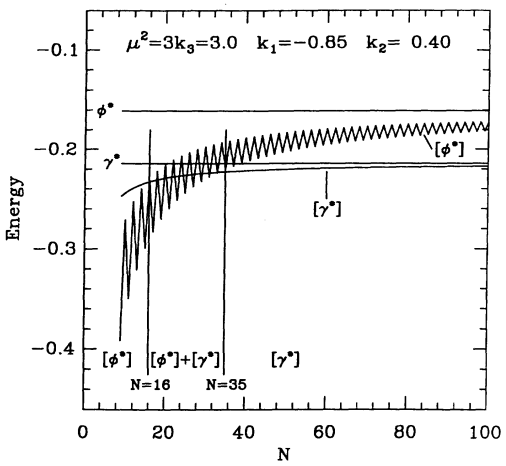

FIG. 6. Plot of the energy of the *strip* structures $[\alpha^*]$, $[\gamma^*]$, and $[\phi^*]$ vs N for $\mu^2=3k_1=3$ and $k_1=-0.85$, $k_2=0.4$. The horizontal straight lines represent the energies of their corresponding *infinite* version α^*, γ^*, and ϕ^*.

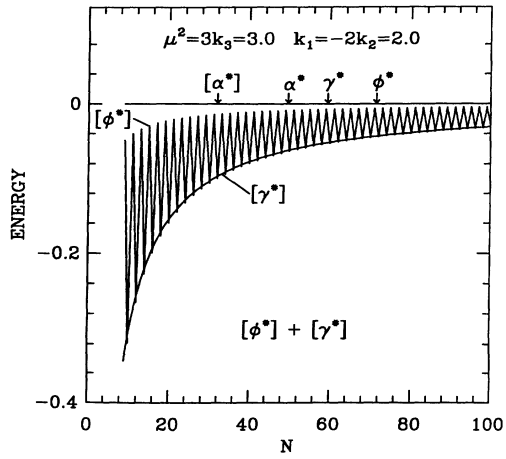

FIG. 7. Plot of the energy of the *strip* structures $[\alpha^*]$, $[\gamma^*]$, and $[\phi^*]$ vs N, for $\mu^2=3k_1=3$ and $k_1=-2k_2=2$. The horizontal straight lines represent the energies of their corresponding *infinite* version α^*, γ^*, and ϕ^*.

does not oscillate. We also note in Figs. 6 and 7 that the energy curves of $[\phi^*]$ and $[\gamma^*]$ versus N progressively approach horizontal straight lines, which represent the energy of their corresponding *infinite* versions, as N increases. Figure 6, performed in the E region (delimited by the small box "E" in the phase diagrams in Figs. 3, 4, and 5), shows—for the parameter set considered—that for the *strip* lattices with size $N<16$, phase $[\phi^*]$ is the ground state. For $16\leq N<35$, $[\phi^*]$ is favorable with respect to $[\gamma^*]$ for odd N values, whereas $[\gamma^*]$ is the ground state for even N values. Consequently, in a powder of strip structures with an average grain size N ranging from 16 to 34 the ground state consists of the mixture $[\gamma^*]+[\phi^*]$ (since in such a powder there are statistically as many grains with size N odd as with size N even). For $N\geq 36$ we see that $[\gamma^*]$ is the single ground state. We note that in the case of $LiIO_3$ this is not in agreement with *experimental* results, which show that γ-$LiIO_3$ always coexists in a mixture with another phase of $LiIO_3$.[22,27] Consequently the parameter regions between $[\alpha^*]$ and $[\gamma^*]$ that are situated towards or in (that is, in the E region and its vicinity) the E region are not appropriate for describing phase transitions.

On the other hand Fig. 7—performed in the D region of the phase diagrams—shows, for the parameter set considered, that $[\gamma^*]$ is the ground state for odd N values, whereas $[\phi^*]$ is the ground state for even N values. That is the reason why $[\phi^*]$ does not appear either in the D region in the phase diagrams in Figs. 3(b), 4(b), and 5(b), or in its vicinity. Consequently in a powder of *strip* structures, for the parameter set considered, $[\gamma^*]$ never appears as a single ground state but always coexists in the mixture $[\gamma^*]+[\phi^*]$ or $[\alpha^*]+[\gamma^*]+[\phi^*]$. We note that in the case of $LiIO_3$ this behavior is not inconsistent with experimental results,[22,27] unlike the behavior in the E region discussed above. Moreover, in general, the whole parameter region of $[\phi^*]$—that is situated towards or in the D region of the phase diagrams [in Figs. 3(a), 4(a), and 5(a)]—is, in fact, the parameter region where the mixture $[\gamma^*]+[\phi^*]$ appears as ground state in a powder of *strip* structures. We stress that this coexistence of several distinct phases in a same region makes the phase diagram for the *strip* lattice quite different from those of *infinite* lattice models and thus shows that the *strip* lattice can better describe some physical states like mixtures of phases or powders with distinct phases.

Furthermore, we see that as N decreases, the domain of existence of $[\gamma^*]+[\phi^*]$ spreads towards the phonon stability region, that is, towards the high-temperature phases, which corresponds to an augmentation of the transition temperatures from $[\alpha^*]$ to $[\gamma^*]$. A similar phenomenon is observed for powders of $LiIO_3$, in which the phase-transition temperatures increase as the grain sizes decrease.[27] Although a comparison between our results and the effects in the real crystal $LiIO_3$ cannot be done in a straightforward manner because of the simplicity of our model with respect to the complexity of the effects in the real material, it is, however, clear that the region of the transition line α^*-γ^* in which the model exhibits some behaviors similar to those one observes in

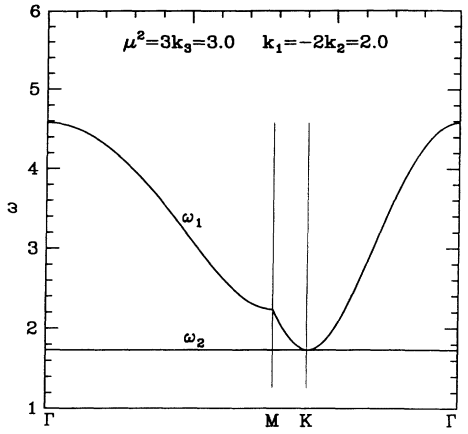

FIG. 8. Plot of phonon dispersion curves for the *infinite* lattice model, for $\mu^2=3k_1=3$ and $k_1=-2k_2=2$ in the directions Γ-M, M-K, and K-Γ, in the Brillouin zone.

$LiIO_3$ reduces to a small parameter region neighboring the set $\mu^2=3k_3$, $k_1=-2k_2=2$ in the D region of the parameter space. We reemphasize that in the other regions of the transition line α^*-γ^* (which is of interest to us) the model exhibits some behaviors that have *never* been observed *experimentally*. Furthermore, it is also interesting to mention that inelastic-neutron-scattering measurements for dispersion curves for optic phonons in α-$LiIO_3$ in the directions Σ and T [$\Sigma=M-\Gamma$, $T=\Gamma-K$, $\Gamma=(0,0,0)$, $K=(2\pi/3, 2\pi/3, 0)$, $M=(0,\pi,0)$] of the Brillouin zone show, within the limit of experimental error, that one of the two frequencies (for the rotation of IO_3^- ions) is essentially constant:[30] $\omega_2=(4.1\pm0.1)10^{12}$ Hz. Such a behavior occurs in the infinite-lattice model solely for the set $k_1=-2k_2=2$ of the transition line α^*-γ^* in Fig. 2 (see Fig. 8), which is situated precisely in the D region.

Our calculations for *strip* phases have revealed the presence of an intermediate phase ϕ^* between α^* and γ^* in the D region of the parameter space. This phase ϕ^* has not been revealed in previous work[4,8] owing to the fact that its domain of existence is reduced to some extremely small parameter regions—essentially *on* the transition line α^*-γ^* in Fig. 2 so that it is not visible in these figures. The observability has become possible because its domain of existence increases as the size of the *strip* lattice decreases, so that ϕ^* becomes clearly visible at smaller *strip* lattice sizes. This result illustrates clearly one of the interests of our *strip calculations* for the theoretical treatment of classical nonlinear lattices. Furthermore, the presence of the phase ϕ^* between α^* and γ^* shows that our *strip calculations*—which consider only the preponderant phenomenon that characterizes the transition α-γ of $LiIO_3$, that is, the rotation of the IO_3^- ions around the c axis of the crystal—gives a theoretical support on the hypothesis of the existence of an intermediate phase of $LiIO_3$ during the transition α-γ. This hypothetical modification of $LiIO_3$ was already postulated in view of some NMR results.[24] In this reference, although the authors do not propose any structure for this hypothetical phase, denoted α'—$LiIO_3$ in Ref. 24, they report some of its essential features suggested by their

diffraction and NMR results, that this phase might be an amorphous, or at least a very divided phase and that its domain of existence is very narrow. We note that these correspond precisely to the main features of our phase ϕ^*, mentioned above. Furthermore, since the transition from α- to γ-$LiIO_3$ involves only a very slight distortion of the Li sublattice,[24] one can conceive that in the first step of this transition the crystal transforms into a phase in which only a quarter of IO_3^- ions of α-$LiIO_3$ have rotated according to the configuration of ϕ^* (see Table II), and the Li sublattice remains unchanged (or becomes very slightly distorted) related to the hexagonal lattice. Then, upon heating, the crystal transforms into γ-$LiIO_3$ according to the mechanism suggested in Ref. 24, briefly discussed below.

Thus, the presence of ϕ^* in our *strip*-lattice phase diagram and its main features suggest its 3D version, which we denote hereafter as ϕ-$LiIO_3$, as a possible phase of $LiIO_3$. We have used here the notation ϕ-$LiIO_3$ instead of α'-$LiIO_3$ used in Ref. 24 just to avoid any confusion with α-$LiIO_3$. Figure 9 shows schematically the projection of the structure of ϕ-$LiIO_3$ onto the *a-b* plane orthogonal to the *c* axis of the crystal, that we obtain by simply applying for each IO_3^- ions of the unit cell the rotational position $\pm\theta$ according to the configuration of ϕ^*. Indeed by calculating the static solutions $q_{n,m,i}$ in the parameter regions, where ϕ^* exists, we find that the absolute value $|q_{n,m,i}|$ is the same for all IO_3^- ions as well in ϕ^* as in α^*, which suggests that $\theta \approx 15°$ in ϕ-$LiIO_3$, as well in α-$LiIO_3$. However, the rotational positions of IO_3^- ions in the very divided phase ϕ-$LiIO_3$ is certainly somewhat different from 15° at the vicinity of the boundaries of the structure because of the extreme sensitivity of ϕ-$LiIO_3$ to the division state of the material. That is precisely what we find by calculating the static solutions $q_{n,m,i}$ for the *strip* structures [ϕ^*].

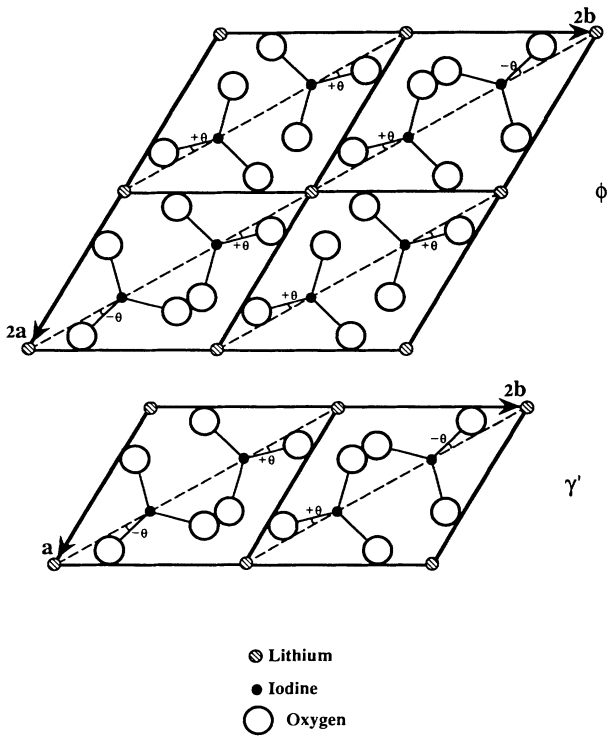

FIG. 9. Projection of the structure ϕ-$LiIO_3$ and γ'—$LiIO_3$ onto the *a-b* plane. Only one unit cell of each phase is represented.

ϕ-$LiIO_3$ possesses eight formula units per unit cell ($Z=8$), and we find that it is space group is $P6_3$. Note that ϕ and α have the same space group. Assuming the existence of the phase ϕ-$LiIO_3$ can allow the explanation, at least partly, of why ϕ-$LiIO_3$ has not yet been directly observed in diffraction experiments, and why Crettez *et al.*[24] have failed to refine the structure of α-$LiIO_3$ from their mixed sample $\alpha+\gamma+\phi$.

We think that a possible explanation is the following: The α and ϕ phases have the same space group, and consequently their diffraction diagrams yield the same Bragg reflection angles and differ solely in the intensity of the reflections owing to the fact that the number of formula units per unit cell differs in two phases. Moreover, since the domain of existence of ϕ is extremely narrow and increases only in the case of extreme division of the crystal, it is clear that the ratio ϕ/α or ϕ/γ in a mixed sample $\alpha+\gamma+\phi$ is very small, and consequently the intensities of the Bragg reflections for ϕ are relatively weak but can become perceptible in powders with very small grain sizes. One can then conceive that Crettez *et al.*[24] have succeeded in determining the structure of γ from the sample $\alpha+\gamma+\phi$ because the space group of ϕ (and α) differs from that of γ, and they have failed to obtain the structure of α because of the presence of ϕ, which acts rather like a *small perturbation* of the intensities of the Bragg reflections of the α phase. However, another possible explanation of their[24] intensity data might involve fragmentation of the crystallite during the transition because of the strains localized at the interface between phases or even the coupling between surface and boundary effects and strains localized at the interface between phases that become extremely important in very divided phases; this shows that, nevertheless, our model oversimplifies the effects in the real material, and that additional theoretical and experimental investigations are required in order to confirm the existence of the phase ϕ-$LiIO_3$.

An important point related to the description of γ-$LiIO_3$ with the 2D model under consideration should now be clarified. In fact, the space group of γ-$LiIO_3$, $Pna2_1$, corresponds to an orthohombic Li sublattice and consequently cannot be rigorously described with the present model. However, the present model can be used to describe the transition from α to γ, since the model takes into account the preponderant phenomenon that characterizes this transition, that is the rotation of IO_3^- ions around the *c* axis of the crystal. Nevertheless in order to avoid any confusion we use for some forthcoming discussions the notation γ' to designate the 3D version of γ^*, in which the Li sublattice is quite hexagonal instead of γ as we did before. The phase γ'-$LiIO_3$, whose projection onto the *a-b* plane is schematically shown in Fig. 9, has been suggested in Ref. 24 as an intermediate step during the transition from α to γ from which the system relaxes into the more energetically favorable phase γ by a

slight distortion of the Li sublattice, small cooperative shifts and small tilts of IO_3^- ions from the c axis. In the first step of the mechanism suggested in Ref. 24 half of IO_3^- ions of α rotate and α transforms into γ'. Assuming the existence of ϕ-$LiIO_3$, one can conceive an intermediate step between α and γ' in which only a quarter of IO_3^- of α rotates, which gives rise to ϕ. Then, upon heating, a quarter of IO_3^- of ϕ rotates and ϕ transforms into γ', and then the system relaxes into γ. This shows that the main steps of mechanism for the transition α-γ suggested in Ref. 24 are preserved in the presence of ϕ-$LiIO_3$.

IV. SUMARY AND CONCLUSION

We have considered in this work the strip version of the two-dimensional hexagonal lattice in the double-quadratic substrate considered in Refs. 4 and 8. Our results show that size effects modify the phonon stability region in the phase diagram of the lattice, which involves a slight or significant modification of the domain of stability of high-temperature phases depending upon the parameter regions. Size effects also involve complete changes for the ground states in some parameter regions, in that some phases appearing in the phase diagram of the *infinite* lattice are not longer the ground states in the *strip* lattices for self-consistency reasons. The *true* 2D phases appear to be much more sensitive to size effects than quasi-1D phases. On the other hand, some other phases appear as ground states solely in the *strip* lattices, which shows that in some parameter regions the *strip* lattices are extremely sensitive to boundary effects even if the boundaries are at large distances apart, which gives rise to divided phases. We have found several 2D divided ground-state phases of the model. The general features of one of them, ϕ^*, suggest a new modification of $LiIO_3$, whose 2D projection is shown in Fig. 9. This result has, of course, to be checked experimentally. The process for directly observing this hypothetical phase from diffraction experiments is in current progress. Furthermore, all results shows that the hexagonal model under consideration qualitatively describes some essential features, and particularly the transition from α- to γ-$LiIO_3$ solely for a very small parameter range neighboring the set $\mu^2=3k_3=3$, $k_1=-2k_2=2$ of the model.

However, it is clear that at the actual stage of the development of theoretical treatments of 2D nonlinear lattice models, one unfortunately cannot yet construct models that accurately describe some interesting properties or effects—such as size effects—for real crystals, which are generally very complicated. In this context our *strip calculations*—which take into account size effects in the theoretical treatment of a 2D nonlinear lattice model—is just a step in the development of more realistic models for real physical systems. An important question that remains to be answered is how size effects manifest themselves in a two-dimensional model with finite size in the two directions of the lattice. Furthermore, a useful extension of the model would be to include the rotations of IO_3^- ions around axes lying in the a-b plane, which could allow us to give an account of β-$LiIO_3$. It would also be interesting to estimate the difficulty of nucleation of γ by computing the energy of the interface between the α^* and γ^* phases in order to provide a more likely explanation of the size effects on the α-γ phase-transition temperature in $LiIO_3$. Finally we would like to point out that we have extensively discussed the case of $LIIO_3$ merely because it provides an example of size effects about which we have extensive experimental data. However the approach that we have presented here to analyze the phase diagrams of a *strip* lattice can be easily extended to other cases. Our analysis suggests that size effects can significantly affect the phase diagram of a lattice and therefore must not be ignored.

ACKNOWLEDGMENTS

The authors would like to thank R. Boesch for a careful reading of the manuscript. The numerical calculations were performed on a Telmat T-Node financed by the CEC Parallel Computing Action No. 4214, and this work was partly supported by the CEC Science program under Contract No. SCI/0299-C (AM).

[1]F. Axel and S. Aubry, J. Phys. C **14**, 5433 (1981).
[2]M. Peyrard and H. Büttner, J. Phys. C **20**, 1535 (1987).
[3]P. Tchofo Dinda and E. Coquet, J Phys. Condens. Matter **2**, 6953 (1990).
[4]P. Tchofo Dinda and E. Coquet, J. Phys. Condens. Matter **3**, 7587 (1991).
[5]H. Büttner and J. Heym, Z. Phys. B **68**, 279 (1987).
[6]P. Tchofo Dinda, doctoral thesis, University of Dijon, 1991.
[7]G. Vlastou-Tsinganos, Ph.D. thesis, University of Crete, 1991.
[8]E. Coquet, M. Peyrard, and H. Büttner, J. Phys. C **21**, 4895 (1988).
[9]G. Vlastou-Tsinganos, N. Flytzanis, and H. Büttner, J. Phys. A **23**, 225 (1990).
[10]G. Vlastou-Tsinganos, N. Flytzanis, and H. Büttner, J. Phys. A **23**, 4553 (1990).
[11]Y. Ishibashi and H. Shiba, J. Phys. Soc. Jpn. **45**, 409 (1978).
[12]Y. Ishibashi, W. Buchleit, and J. Petersson, Solid State Commun. **38**, 1277 (1981).
[13]M. N. Baretto, P. Lederer, and J. P. Jamet, Phys. Rev. B **28**, 3994 (1983).
[14]G. Dénès, J. Solid State Chem. **37**, 16 (1981).
[15]R. Marx, Phys. Rep. **125**, 1 (1985).
[16]Michael E. Fisher and Michael N. Barber, Phys. Rev. Lett. **28**, 1516 (1972).
[17]Arthur E. Ferdinand and Michael E. Fisher, Phys. Rev. **185**, 832 (1969).
[18]John W. Essam and Michael E. Fisher, J. Chem. Phys. **38**, 802 (1962).
[19]K. Binder and P. C. Hohenberg, Phys. Rev. B **9**, 2194 (1974).
[20]K. Binder, Ferroelectrics **73**, 43 (1987).

[21]Y. Imry and D. Bergman, Phys. Rev. A **3**, 1416 (1971).
[22]J. Pannetier, E. Coquet, J. Bouillot, and J. M. Crettez, C. R. Acad. Sci. Paris, **299**(9), Série II, 541 (1984).
[23]J. M. Crettez, E. Coquet, B. Michaux, J. Pannetier, P. Orlans, A. Nonat, and J. C. Mutin, Physica B **144**, 277 (1987).
[24]J. M. Crettez, E. Coquet, J. Pannetier, J. Bouillot, and M. Durand-Le-Floch, J. Solid State Chem. **56**, 133 (1985).
[25]E. Coquet, J. M. Crettez, J. Pannetier, J. Bouillot, and J. C. Damien, Acta Crystallogr. B **39**, 408 (1983).
[26]S. Matsumura, Mater. Res. Bull. **6**, 469 (1971).
[27]J. M. Crettez, doctoral thesis, University of Dijon, 1984.
[28]V. Lemos, J. Mendez Filho, F. E. A. Melo, R. S. Katiyar, and F. Cerdeira, Phys. Rev. B **28**, 2985 (1983).
[29]J. K. Liang, G. H. Rao, and Y. M. Zhang, Phys. Rev. B **39**, 59 (1989).
[30]J. Bouillot and E. Coquet (unpublished).
[31]B. Carnahan, H. A. Luther, and J. O. Wilkes, *Applied Numerical Methods* (Wiley, New York, 1976), pp. 441–442.
[32]G. Caboche, doctoral thesis, University of Dijon, 1991.